Articles

Ab initio Calculation and Kinetic Study for the Abstraction Reaction of H with $SiHCl_3$

ZHANG, Qing-Zhu(张庆竹) **WANG, Shao-Kun(王少坤)** **GU, Yue-Shu*** **(顾月姝)**
School of Chemistry and Chemical Engineering, Shandong University, Jinan, Shandong 250100, China

The mechanism of the reaction of H with $SiHCl_3$ has been investigated at high level of *ab initio* molecular orbital theory. Theoretical analysis provides a conclusive evidence that the main process occurring in this reaction is the hydrogen abstraction from the Si—H bond, the abstraction of Cl has higher barrier and is difficult to react. The kinetics has been studied using canonical variational transition-state theory (CVT) with small curvature tunneling effect (SCT) correction. The rate constants have been calculated over a wide temperature range of 200—3000 K. The CVT/SCT rate constants exhibit typical non-Arrhenius behavior, a three-parameter rate-temperature formula is fitted as follows:
$k(T) = (3.24 \times 10^{-19}) T^{2.30} \exp(-250/T)$ [in unit of mL/(molecule·s). The calculated CVT/SCT rate constants match well with the experimental values.

Keywords Trichlorosilane, abstraction reaction, variational transition state

Trichlorosilane is an important material in plasma Chemical Vapor Deposition (CVD) and in semiconductor device process.[1-4] The reaction of trichlorosilane with atomic hydrogen, the simplest free-radical species, has drawn considerable attention; kinetic parameters for H-atom reaction are desirable not only to provide an uncomplicated probe for chemical reactivity but also to be helpful for a more extensive use of trichlorosilane. However, the work for the direct hydrogen abstraction from trichlorosilane was very limited. Only one experimental study was reported. In 1989, Arthur[5] obtained the Arrhenius formula of the reaction of $SiHCl_3$ with atomic H over the temperature range of 290—482 K: $k(T) = (0.27 \pm 0.02) \times 10^{-11} \exp[(-1111 \pm 24)/T]$ [in mL/(molecule·s)]. To our knowledge, there is no theoretical study on this reaction.

In this paper, we present the theoretical study on this reaction. Several features of this work are the following: (1) the reaction mechanism has been revealed at high level of *ab initio* molecular orbital theory. (2) the energy profile surface has been calculated at the G3MP2[6] theory. (3) the rate constants have been obtained using canonical variational transition-state theory with small curvature tunneling effect (CVT/SCT) over a wide temperature range of 200—3000 K. (4) the non-Arrhenius expression has been fitted. (5) the results of CVT/SCT calculation are compared with experimental values.

Computational methods

Ab initio calculations have been carried out using Gaussian 94 programs.[7] The geometries of the reactant, transition states and products have been optimized at the UMP2(FULL)/6-31G(d) level. The vibrational frequencies have been calculated at the same level of theory in order to determine the nature of different stationary points and the zero point energy (E_{ZP} scaled by a factor of 0.93). The number of the imaginary frequency (0 or 1) confirms whether a bound minimum or a transition state has been located. The intrinsic reaction coordinate (IRC) calculation confirms that the transition state connects the designated reactants and products. At the UMP2(FULL)/6-31G(d) level, the minimum energy path (MEP) has been obtained with a gradient step size

* E-mail: guojz@icm.sdu.edu.cn
Received May 8, 2001; revised September 24, 2001; accepted October 17, 2001.
Project supported by the Research Fund for the Doctoral Program of the Ministry of Education of China (No.1999042201).

of 0.05 amu$^{1/2}$ bohr in mass-weighted cartesian coordinate, and the force constant matrices of the stationary and the selected non-stationary points near the transition state along the MEP have been also calculated. Because the shape of the MEP is important for the calculation of the rate constants, the energies of the stationary points and the non-stationary points are refined by the G3MP2 theory.

The CVT is based on the idea of varying the dividing surface along a reference path to minimize the rate constant. In this paper, the theoretical rate constant has been obtained using the CVT plus SCT correction. All the kinetic calculations have been carried out using the Polyrate 7.8 program.[8]

Results and discussion

Reaction mechanism

The optimized geometries of the reactants, transition states, and products are shown in Fig. 1. The vibrational frequencies are listed in Table 1. The total energies and the relative energies for all species are summarized in Table 2.

It is worth stating the reliability of the calculations in this work. Since unrestricted Hartree-Fock (UHF) reference wave functions are not spin eigenfunctions for open-shell species, the expectation values of $< S^2 >$ were monitored in the UMP2(FULL)/6-31G(d) optimization. The values of $< S^2 >$ are always in the range of 0.750—0.845 for doublet. After spin annihilation, the value of $< S^2 >$ is 0.750, where 0.750 is the exact value for a pure doublet. Thus, spin contamination is not severe. This suggests that a single determinant reference wave function for this system be suitable for the level of theory used in the optimization.[10] As shown in Fig. 1, the geometric parameters of $SiHCl_3$ and H_2 are in good agreement with the available experimental values. From this result, it might be inferred that the same accuracy could be expected for the geometries of other species. As can be seen from Table 1, the scaled vibrational frequencies of the reactant agree well with the experimentally observed fundamentals, and the relative error is less than 6%.

As mentioned above, the reaction of $SiHCl_3$ with H can occur via two channels: the hydrogen abstraction and the chlorine abstraction, namely:

$$H + SiHCl_3 \longrightarrow H_2 + SiCl_3 \quad (1)$$

$$H + SiHCl_3 \longrightarrow HCl + SiHCl_2 \quad (2)$$

In the transition state TS_1 structure, the forming H—H bond of 0.103 nm is 39.19% longer than the equilibrium value of the H_2, while the breaking Si—H bond is stretched 12.24% from the reactant to the transition state. Therefore, TS_1 is reactant like, and the hydrogen abstraction reaction will proceed via an early transition state. H atom attacks linearly the H atom of $SiHCl_3$, and the transition state TS_1 has C_{3v} symmetry. In the transition state TS_2 structure, the forming H—H bond of 0.148 nm is 15.63% longer than the equilibrium value of the HCl, while the breaking Si—Cl bond is elongated from 0.203 nm in the reactant to 0.236 nm in TS_2. H atom attacks one of the three Cl atoms of $SiHCl_3$ with a slightly bent orientation angle of 175.8°. The TS_2 has C_s symmetry.

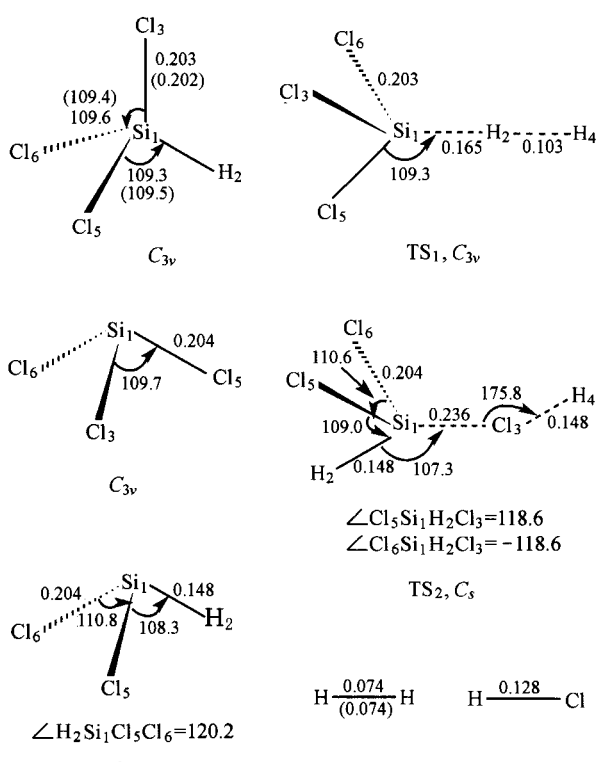

Fig. 1 Optimized geometries for the stationary points. The distance is in nm and the angle is in degree. The values in parenthesis are experimental data.[9]

Table 1 Scaled vibrational frequencies (in cm^{-1}) of the reactant, transition states and products (The values in parenthesis are the experimental results[11,12])

Species	$SiHCl_3$	TS_1	$SiCl_3$	TS_2	$SiHCl_2$	H_2	HCl
Frequency	2236(2261)	1137	574	2226	2145	4218(4404)	2835
	787(811)	920	574	747	739		
	787(811)	920	459	682	645		
	583(600)	485	235	515	564		
	583(600)	485	159	499	499		
	475(499)	382	159	426	172		
	244(254)	194		354			
	166(176)	163		354			
	166(176)	163		166			
		133		128			
		133		91			
		-1598		-1510			

In order to choose a reliable theory level to calculate the energy, the bond dissociation energies were calculated for the $SiCl_3$—H. The values at UMP2(FULL)/6-31G(d), UQCISD(T)/6-31G(d) and G3MP2 levels are 360.75, 364.20, 382.41 kJ/mol, respectively. The experimental value[13] is 382.42 kJ/mol. The experiments gave the spectrum dissociation energy, and so the calculated dissociation energies were corrected for the E_{ZP}. It can be seen that the calculated results at the G3MP2 level are in good agreement with the experimental value. Both the UMP2 and the UQCISD(T) levels underestimate the bond dissociation energy. So the G3MP2 theory is a good choice to calculate accurate energies for the title system.

Table 2 The total energies (E, in hartree) and the relative energies (ΔE, in kJ/mol) at the G3MP2 theory level.

Species	E	ΔE
$SiHCl_3$ + H	-1669.55848	0.00
TS_1	-1669.55195	17.16
TS_2	-1669.52861	78.44
$SiCl_3$ + H_2	-1669.58208	-61.96
$SiHCl_2$ + HCl	-1669.55489	9.43

The total energy and the relative energy of the reactant, transition states, and the product at the G3MP2 theory level are shown in Table 2. The potential barrier of the hydrogen abstraction is 17.16 kJ/mol, while the potential barrier of the chlorine abstraction is 78.44 kJ/mol. The latter is much higher than the former. The hydrogen abstraction is exothermic reaction, while the chlorine abstraction is endothermic reaction. So the chlorine abstraction is difficult to react, and the hydrogen abstraction is the main channel. Therefore, this paper has only mainly discussed the kinetic nature of the hydrogen abstraction in the following section.

Kinetic calculation

The MEP of the hydrogen abstraction was calculated at the UMP2(FULL)/6-31G(d) level by the IRC theory, and the energies of the MEP were refined by G3MP2//UMP2 method. As functions of the intrinsic reaction coordinate s, the classical potential energy V_{MEP} and the ground-state vibrational adiabatic potential energy V_a^G of the hydrogen abstraction reaction are shown in Fig. 2. From $s = -\infty$ to -2.0 $amu^{1/2}$ bohr, the potential curves change very slowly. From $s = -2.0$ $amu^{1/2}$ bohr, the curves increase gradually and decrease quickly on passing the transition state. The classical potential energy curve reaches the value of -61.96 kJ/mol after $s = 2.0$ $amu^{1/2}$ bohr, which is the calculated nonscaled reaction enthalpy. It can be seen that the V_{MEP} and V_a^G curves are similar in shape, and their maximum positions are almost the same at the G3MP2//UMP2 level. So the E_{ZP}, which is the difference of V_a^G and V_{MEP} is practically constant as s varies. In order to analyze this behavior in greater detail, the variation of

the generalized normal mode vibrational frequencies of the hydrogen abstraction reaction are shown in Fig. 3.

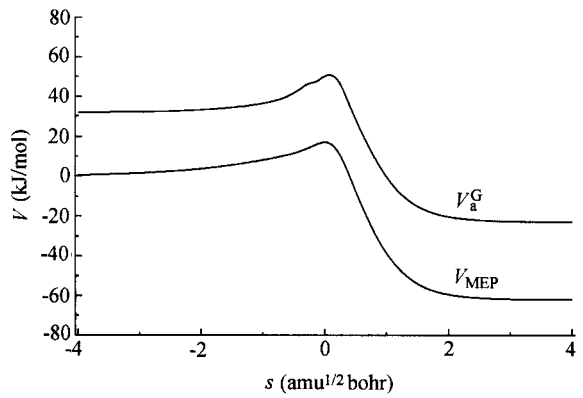

Fig. 2 Changes of V_{MEP} and V_a^G along the reaction coordinate s.

In the negative limit of s, the frequencies are associated with the reactant, while in the positive limit of s, the frequencies are associated with the products. In the reactant limit, only nine frequencies are nonzero, while in the product limit, seven frequencies are nonzero. It can be seen from Fig. 3 that mode 1 drops dramatically near the saddle point. This behavior is known to be typical of hydrogen transfer reaction.[14] A priori, this drop should cause a considerable fall in the E_{ZP} near the saddle point. However, the modes 10 and 11 begin to appear from $s = -0.1$ amu$^{1/2}$ bohr and reach their maxima in the saddle point, and modes 2 and 3 have a rising in the transition state zone. These behaviors compensate the fall of the mode 1. As a result, the V_{MEP} and V_a^G curves are similar in shape. This analysis indicates that the variational effects will be small or almost negligible for this reaction.

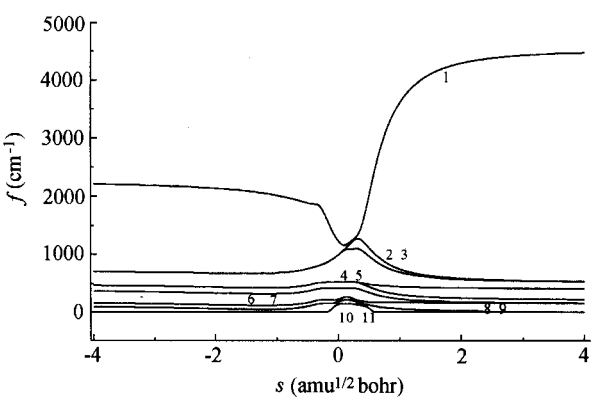

Fig. 3 Changes of frequencies of vibrational modes along the reaction coordinate s.

The CVT with the SCT correction, which has been successfully performed for several reactions,[15-16] is an effective method to calculate the rate constant. This paper used this method to calculate the rate constant of the title reaction. In order to calculate the rate constant, 30 points have been selected near the transition state region along MEP—15 points in the reactant zone and 15 points in the product zone. Fig. 4 shows the calculated CVT/SCT rate constant k of the hydrogen abstraction and experimental values against the reciprocal of the temperature.

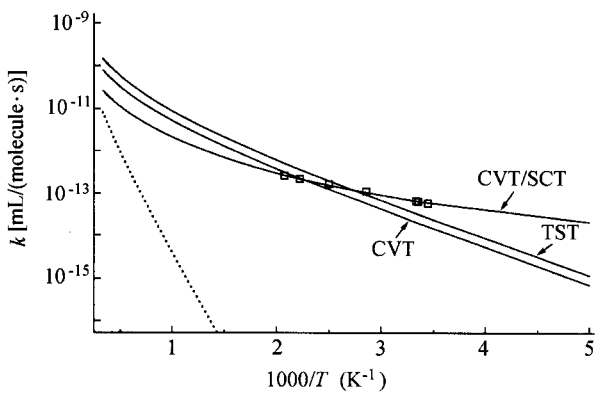

Fig. 4 Rate constants as functions of the reciprocal of the temperature (K) over the temperature range of 200—3000 K, □ being the experimental values.

The experimental values in Fig. 4 have been obtained from the Arrhenius expression fitted by Arthur.[5] It can be seen that the calculated CVT/SCT rate constants are in good agreement with the experimental values. It means that the CVT/SCT method is an effective approach to calculate the rate constants.

For the purpose of comparison, both the conventional transition state theory (TST) and the canonical variational transition state theory (CVT) are shown in Fig. 4. It is seen that the values of TST rate constant and those of CVT rate constant are nearly the same, which enables us to conclude that the variational effect for the calculation of the rate constant is small.

In the lower-temperature range from 200—400 K, the CVT rate constants are much smaller than those of CVT/SCT, which means that in the lower-temperature the quantum tunneling effect is significant. For example, at 298 K, the CVT rate constant is 7.10×10^{-16} mL/(molecule·s), while the CVT/SCT rate constant is 2.06×10^{-14} mL/(molecule·s). The latter is 30.47

times larger than the former. In the temperature range of 450—1000 K, the difference between the CVT rate constant and the CVT/SCT rate constant is small, which means that the tunneling effect plays an unimportant role in the calculation of the rate constant over this temperature range. However, with the temperature increasing, the CVT/SCT rate constants are smaller than the CVT values. For example, at 3000 K, the CVT rate constant is 8.06×10^{-11} mL/(molecule·s), while the CVT/SCT rate constant is 2.69×10^{-11} mL/(molecule·s). It means that the transmission coefficient $\kappa_{SCT} < 1$, over the temperature range of 1100—3000 K.

It is obvious that the CVT/SCT rate constant exhibits typical non-Arrhenius behavior. The CVT/SCT rate constants over the temperature range of 200—3000 K are fitted by a three-parameter formula and given in unit of mL/(molecule·s) as follows:

without tunneling

$$k(T) = (7.96 \times 10^{-16}) T^{1.58} \exp(-1586/T),$$

or, including tunneling

$$k(T) = (3.49 \times 10^{-19}) T^{2.30} \exp(-250/T).$$

Our fitted expression is different from that of Arthur.[5] It is because that our expression was fitted over a wide temperature range of 200—3000 K, which exhibits non-Arrhenius behavior. However, the expression of Arthur was fitted over a narrow temperature range of 290—482 K, which exhibits typical Arrhenius behavior.

In order to compare with the CVT/SCT rate constants of the hydrogen abstraction, the CVT/SCT rate constants of the chlorine abstraction are also shown in Fig. 4 (the imaginary line). It can be seen that the rate constants of the chlorine abstraction are much smaller than those of the hydrogen abstraction at the whole studied temperature range, and the contribution of the chlorine abstraction to the total rate constant can be negligible. For example, at 200 K, the CVT/SCT rate constant of the hydrogen abstraction is 1.6×10^{14} times larger than that of the chlorine abstraction, and at 3000 K, the CVT/SCT rate constant of the hydrogen abstraction is 10 times larger than that of the chlorine abstraction. Therefore, the hydrogen abstraction is the sole channel for the reaction of H with $SiHCl_3$, which is consistent with the above analysis.

Conclusion

This work has calculated the rate constant for the reaction of H with $SiHCl_3$ using CVT with SCT correction. The calculated values have been found to be in agreement with the experimental results. From the above study the following conclusions can be drawn:

1. The hydrogen abstraction is the sole channel for the reaction of H with $SiHCl_3$.

2. The variational effect is small for the calculation of the rate constant.

3. The CVT/SCT rate constant exhibits typical non-Arrhenius behavior.

References

1 Beaucarne, G.; Poortmans, J.; Caymax, M.; Nijs, J.; Mertens, R. *Mater. Res. Soc. Symp. Proc.* **1998**, *485*, 89.

2 Bisch, C.; Llauyo. G.; Wang, Y. B. *J. Appl. Phys.* **1998**, *3*, 47.

3 Hiroyuki, N.; Kuniaki, Y.; Yukitaka, N. *Nippon Kessho Seicho Gakkaishi* **1998**, *25 A*, 109.

4 Kamimura, K.; Miwa, T.; Sugiyama, T.; Ogawa, T.; Nakao, M.; Onuma, Y. *Inst. Phys. Conf. Ser.* **1996**, *142*, 825.

5 Arthur, N. L.; Potzinger, P.; Reimann, B.; Steenbergen, H. P. *J. Chem. Soc., Faraday Trans. 2* **1989**, *85*, 1447.

6 Curtiss, L. A.; Redfern, P. C.; Raghavachari, K.; Rassolov, V.; Pople, J. A. *J. Chem. Phys.* **1999**, *110*, 4703.

7 Frisch, M. J.; Trucks, G. W.; Schlegel, H. B.; Gill, P. W. M.; Johnson, B. G.; Robb, M. A.; Cheeseman, J. R.; Keith, T. A.; Petersson, G. A.; Montgomery, J. A.; Raghavachari, K.; Allaham, M. A.; Zakrzewski, V. G.; Ortiz, J. V.; Foresman, J. B.; Cioslowski, J.; Stefanov, B. B.; Nanayakkara, A.; Challacombe, M.; Peng, C. Y.; Ayala, P. Y.; Chen, W.; Wong, M. W.; Andres, J.; Replogle, E. S.; Gomperts, R.; Martin, R. L.; Fox, D. J.; Binkley, J. S.; Defrees, D. J.; Baker, J.; Stewart, J. P.; Head-Gordon, M.; Gonzales, C.; Pople, J. A. *GAUSSIAN*94, Revision E.1, Gaussian, Pittsburgh, PA, **1995**.

8 Steckler, R.; Chuang, Y. Y.; Fast, P. L.; Corchade, J. C.; Coitino, E. L.; Hu, W. P.; Liu, Y. P.; Lynch, G. C.; Nguyen, K.; Jackells, C. F.; Gu, M. Z.; Rossi,

I.; Clayton, S.; Melissas, V.; Garrett, B. C.; Isaacson A. D.; Truhlar, D. G. *Polyrate* 7.8 *Version*, University of Minnesota, Minneapolis, **1997**.

9 Mockler, R.; Bailey, J. H.; Lordy, W. *J. Chem. Phys.* **1953**, *21*, 1710.

10 Liu, R.; Francisco, J. S. *J. Phys. Chem. A* **1998**, *102*, 9869.

11 Delwaulle, M. L.; Francois, M. F. *Comptes Rendus* **1949**, *228*, 1007,

12 Burger, H.; Ruoff, A. *Spectrochim. Acta* **1970**, *26*, 1449.

13 Wu, Y. D.; Wong, C. L. *J. Org. Chem.* **1995**, *60*, 821.

14 Corchado, J. C.; Espinosa-Garcia, J. *J. Chem. Phys.* **1996**, *105*, 3160.

15 Yin, H. M.; Yang, B. H.; Han, K. L.; He, G. Z.; Guo, J. Z.; Liu, C. P.; Gu, Y. S. *Phys. Chem. Chem. Phys.* **2000**, *2*. 5093.

16 Yu, X.; Li, S. M.; Xu, Z. F.; Li, Z. S.; Sun, C. C. *Chem. Phys. Lett.* **2000**, *320*, 123.

(E0105086FZ. DONG, L. J.)